Eur. Phys. J. A **13**, 377–382 (2002)

THE EUROPEAN PHYSICAL JOURNAL A

Enhanced electron screening in d(d, p)t for deuterated Ta*

F. Raiola[1], P. Migliardi[1], G. Gyürky[2], M. Aliotta[1,a], A. Formicola[1], R. Bonetti[3], C. Broggini[4], L. Campajola[5], P. Corvisiero[6], H. Costantini[6], J. Cruz[7], A. D'Onofrio[8], Z. Fülöp[2], G. Gervino[9], L. Gialanella[5], A. Guglielmetti[3], G. Imbriani[5], C. Gustavino[10], A.P. Jesus[7], M. Junker[10], R.W. Kavanagh[11], P.G.P. Moroni[6], A. Ordine[5], J.V. Pinto[7], P. Prati[6], V. Roca[5], J.P. Ribeiro[7], D. Rogalla[1], C. Rolfs[1,b], M. Romano[5], F. Schümann[1], D. Schürmann[1], E. Somorjai[2], F. Strieder[1], F. Terrasi[8], H.P. Trautvetter[1], and S. Zavatarelli[6]

[1] Institut für Physik mit Ionenstrahlen, Ruhr-Universität Bochum, Bochum, Germany
[2] Atomki, Debrecen, Hungary
[3] Dipartimento di Fisica, Università di Milano and INFN, Milano, Italy
[4] INFN, Padova, Italy
[5] Dipartimento di Scienze Fisiche, Università Federico II and INFN, Napoli, Italy
[6] Dipartimento di Fisica, Università di Genova and INFN, Genova, Italy
[7] Centro de Fìsica Nuclear, Universidade de Lisboa, Lisboa, Portugal
[8] Dipartimento di Scienze Ambientali, Seconda Università di Napoli, Caserta and Napoli, Italy
[9] Dipartimento di Fisica Sperimentale, Università di Torino and INFN, Torino, Italy
[10] Laboratori Nazionali del Gran Sasso dell'INFN, Assergi, Italy
[11] California Institute of Technology, Pasadena, CA, USA

Received: 21 December 2001
Communicated by D. Schwalm

Abstract. The recent observation of a large electron screening effect in the d(d, p)t reaction using a deuterated Ta target has been confirmed using somewhat different experimental approaches: $U_e = 309 \pm 12$ eV for the electron screening potential energy. The high U_e value arises from the environment of the deuterons in the Ta matrix, but a quantitative explanation is missing.

PACS. 25.10.+s Nuclear reactions involving few-nucleon systems – 25.45.-z ^{2}H-induced reaction – 95.30.-k Fundamental aspects of astrophysics

1 Introduction

In the extrapolation of the cross-section $\sigma(E)$ of a charged-particle–induced nuclear reaction to astrophysical energies E (all energies are given in the centre-of-mass system except where quoted differently) one uses the equation [1]

$$\sigma(E) = S(E)E^{-1}\exp(-2\pi\eta)\,, \qquad (1)$$

where $\eta = 2\pi Z_1 Z_2 e^2/hv$ is the Sommerfeld parameter (in standard notations) and $S(E)$ is the astrophysical $S(E)$ factor. The equation assumes that the Coulomb potential of the target nucleus and projectile is that resulting from bare nuclei. However, for nuclear reactions studied in the laboratory, the target nuclei and the projectiles are usually in the form of neutral atoms or molecules and ions, respectively. The electron clouds surrounding the interacting nuclides act as a screening potential: the projectile effectively sees a reduced Coulomb barrier, both in height and radial extension. This, in turn, leads to a higher cross-section for the screened nuclei, $\sigma_s(E)$, than would be the case for bare nuclei, $\sigma_b(E)$. There is, in fact, an enhancement factor [2],

$$f_{lab}(E) = \sigma_s(E)/\sigma_b(E) = E(E+U_e)^{-1}\exp(\pi\eta U_e/E) \geqslant 1\,, \qquad (2)$$

where U_e is an electron screening potential energy. In the adiabatic limit (U_{ad}), this energy can be calculated, for example, from the difference in atomic binding energies between the compound atom and the projectile plus the target atoms of the entrance channel. According to eq. (2), the enhancement factor $f_{lab}(E)$ increases exponentially with decreasing energy. Note that for a stellar plasma, the value of the bare cross-section $\sigma_b(E)$ must be known because the screening in the plasma will be quite different from that in the laboratory nuclear-reaction studies, *i.e.* $\sigma_{plasma}(E) = f_{plasma}(E)\sigma_b(E)$, where the plasma enhancement factor $f_{plasma}(E)$ must be explicitly included for each situation. A good understanding of electron screening effects in the laboratory is needed to arrive at reliable $\sigma_b(E)$ data at low energies.

[a] Alexander von Humboldt Fellow.
[b] e-mail: rolfs@ep3.ruhr-uni-bochum.de

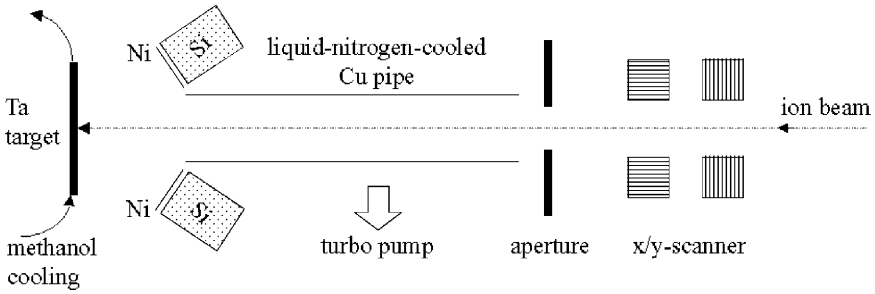

Fig. 1. Schematic diagram of the experimental setup.

Experimental studies of reactions involving light nuclides have shown the expected exponential enhancement of the cross-section at low energies. However, the observed enhancements were in all cases significantly larger than could be accounted for from the adiabatic limit $U_{\rm ad}$: for example, using windowless gas targets one found $U_{\rm e} = 25 \pm 5$ eV ($U_{\rm ad} = 14$ eV) for the reaction d(d, p)t [3] and $U_{\rm e} = 219 \pm 7$ eV ($U_{\rm ad} = 120$ eV) for the reaction ^{3}He(d, p)^{4}He [4]. The discrepancy between $U_{\rm e}$ and $U_{\rm ad}$ is presently not understood (for details, see review article [5]). The situation is disturbing because if the effects of electron screening are not understood under laboratory conditions, they are most likely to be not fully understood in a stellar plasma. An improved understanding of laboratory electron screening may help eventually to improve the corresponding understanding of electron screening in stellar plasmas, such as in our sun. It is in the nature of astrophysics that many of the processes and most of the objects one tries to understand are physically inaccessible. Thus, it is important that those aspects that can be studied in the laboratory be rather well understood. The electron screening project addresses one such aspect.

Recently, the electron screening effect on the d(d, p)t reaction has been studied in the metals Al, Zr, and Ta [6], where deuterated metals were produced via implantation of low-energy deuterons. The resulting $S(E)$ data show an exponential enhancement according to eq. (2), however the extracted $U_{\rm e}$ values ($U_{\rm e} = 190 \pm 15$, 297 ± 8, and 322 ± 15 eV for Al, Zr, and Ta, respectively) are about one order of magnitude larger than the value found in the corresponding gas-target experiment as well as that predicted from $U_{\rm ad}$. An anomalous enhancement was reported earlier [7] for deuterated Pd ($U_{\rm e} = 250 \pm 15$ eV) and a deuterated Au/Pd/PdO multilayer ($U_{\rm e} = 601 \pm 23$ eV), while deuterated Ti and Au exhibited a normal ("gaseous") enhancement: $U_{\rm e} = 36 \pm 11$ and 23 ± 11 eV, respectively. In order to test in part these surprising results, we report on the study of the reaction d(d, p)t for deuterated Ta using somewhat different experimental approaches.

2 Equipment and procedures

The 100 kV accelerator [8] of the Dynamitron-Tandem-Laboratorium at the Ruhr-Universität Bochum provided atomic (D_1^+) and molecular (D_3^+) deuteron beams in the energy range $E_{\rm d} = 4$ to 100 keV, with a particle current of 60 μA at the lowest energy. The absolute beam energy was known to a precision of 3×10^{-4}, which leads to a negligible uncertainty in the d(d, p)t cross-section (0.7% at the lowest energy).

The beam passed through the slits of the analysing magnet (25 mm width) and an aperture (8 mm diameter), which defined the beam direction (2.5 m distance between the slits and the aperture). The aperture was placed at a 46 cm distance from the target (fig. 1). The beam was focused on the target into a spot of about 15 mm diameter: at the lower energies ($E_{\rm d} \leqslant 50$ keV), the beam transmission to the target was about 50% leading to the above spot size; at higher energies, the transmission was 100% and the above spot size was achieved by scanning the beam over the aperture using x- and y-scanners (fig. 1) operated at incommensurable frequencies, whereby the average beam current on the target was reduced by 10%. The procedure was tested using a beam viewer at the target position. The 0.1 mm thick Ta target (50 mm diameter, with direct methanol cooling —at -10°C— applied to the target) was oriented with its normal antiparallel to the beam direction. A liquid-nitrogen–cooled Cu tube (41 cm length, 2.7 cm inner diameter) extended from near the aperture to within 5 cm of the target. With this tube and a turbo pump (450 l/s pumping speed) carbon-buildup on the target was minimised (pressure in the target chamber $= 2 \times 10^{-8}$ mbar). The aperture, the Cu tube, and the target plus target chamber (17 cm diameter, 20 cm length) were electrically insulated.

Four Si detectors (active area = 600 mm^2, effective thickness = 100 μm) were installed at a laboratory angle, $\theta = 130°$, around the beam axis (fig. 1) at a distance of 5 cm from the target and covered with a 0.75 μm thick Ni foil to stop the intense flux of elastically scattered particles. In this arrangement the summed number of counts of the 4 detectors for protons or tritons from d(d, p)t (fig. 2) was nearly independent (to within 1.4%) of the actual location and diameter of the beam spot on target, as tested with an α-source placed at the target position. Using this calibrated α-source, the total solid angle of the 4 detectors was determined to be $\Omega = 0.0689 \pm 0.0009$, consistent with geometry. The detectors were electrically insulated from the target chamber. The target together with the chamber and the detector holders (including the Ni foils) formed a Faraday cup for beam integration. A negative voltage of

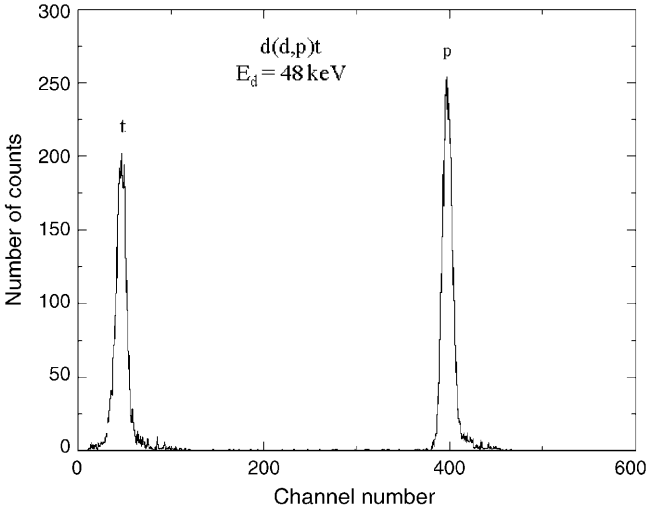

Fig. 2. Sample spectrum obtained with a Si detector (in the setup shown in fig. 1) at $E_{\rm d} = 48$ keV: the proton and triton groups from the d(d, p)t reaction are identified.

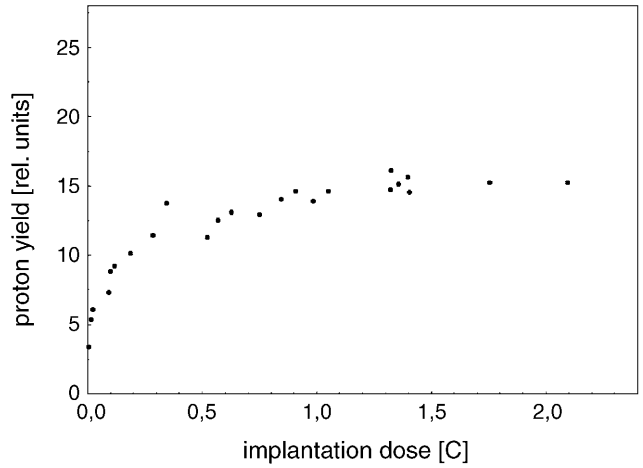

Fig. 3. Proton yield of d(d, p)t as function of deuteron implantation charge in Ta.

200 V was applied to the Cu tube for suppression of secondary electrons. We estimate that the beam current was measured with a precision of about 3%.

The deuterated Ta target was produced in the following way. A fresh Ta foil was bombarded with 10 keV deuterons, whereby the deuterons were scanned over the target area leading to a 20% current reduction compared to the unscanned case; thus, an area somewhat larger than 15 mm diameter was implanted. The proton yield of the d(d, p)t reaction (fig. 2) was recorded as a function of implantation charge: the yield (fig. 3) reached a saturation level after a charge of about 1 Cb, *i.e.* a stoichiometry $\mathrm{Ta}_x\mathrm{D}$ has been produced near the surface of the Ta sheet. Calculations using SRIM [9] indicated that a nearly homogeneous deuteron distribution was formed from the surface down to the range of 10 keV deuterons. The procedure was repeated at higher deuteron energies (up to $E_{\rm d} = 100$ keV), where in each case a saturation level was observed. The deuterated Ta sheet should thus represent an infinitely thick target for the incident deuterons. This expectation was tested via the Elastic-Recoil-Detection Analysis (ERDA, [10]) at the accelerators in Lisboa, München, and Bochum: the deuteron distribution was uniform within 10% from the surface of the Ta sheet down to depths beyond the range of the implanted deuterons, apparently due to a rapid diffusion of D in Ta.

In one run, the deuteron beam was steered away from the target using the x- and y-scanners (fig. 1) in order to search for possible neutral deuterons: no events from d(d, p)t were observed leading to a beam flux ratio $I_{\rm neutral}/I_{\rm charged} < 0.2\%$. In another run, the currents of the D_1^+, D_2^+ and D_3^+ beams after the analysing magnet were compared with that of H_1^+ leading to a contamination of the D_1^+ beam with a H_2^+ beam of at most 1%, which was neglected.

3 Formalism and data analysis

For an incident deuteron energy E_0 and an effective stopping power $\varepsilon_{\rm eff}(E)$ for the $\mathrm{Ta}_x\mathrm{D}$ target, the observed number of counts in the proton peak (fig. 2) of all 4 Si detectors, $N(E_0, \theta)$, is related to the d(d, p)t cross-section $\sigma(E)$ via the equation [1]

$$N(E_0,\theta) = N_{\rm p}\Omega \int_0^{E_0} K_\Omega(E,\theta) W(E,\theta) \sigma(E) \varepsilon_{\rm eff}(E)^{-1} {\rm d}E\,, \tag{3}$$

where $N_{\rm p}$ is the number of incident projectiles. The transformation of solid angle between the center-of-mass system and the laboratory system is described by $K_\Omega(E,\theta)$ and the angular distribution by $W(E,\theta)$. The differential reaction yield of an infinitely thick target is then given by

$$Y^\infty(E_0,\theta) = N(E_0,\theta)/N_{\rm p}\,. \tag{4}$$

An excitation function for $Y^\infty(E_0,\theta)$ was obtained, in up to 13 runs, at $E_0 \equiv E_{\rm d} = 7$ to 100 keV using an atomic beam D_1^+ and at $E_{\rm d} = 4$ to 30 keV using a molecular beam D_3^+, with energy steps $\Delta E_{\rm d}$ varying between 0.5 keV at the low energies and 2 keV at the high energies. The resulting $Y^\infty(E_0,\theta)$ values obtained in one run with the atomic beam are illustrated in fig. 4.

The ratio of the number of counts in the triton peak relative to those in the proton peak (fig. 2) decreased from 0.95 at $E_{\rm d} = 10$ keV to 0.87 at $E_{\rm d} = 100$ keV, consistent with expectation from the product $K_\Omega(E,\theta)W(E,\theta)$ (*e.g.*, $= 0.95$ at $E_{\rm d} = 10$ keV).

The D_3^+ molecular beam breaks up at the target surface leading to an energy spread $\Delta E_{\rm d}$ of the resulting atomic deuteron beam due to the effects of Coulomb explosion of the molecular beam, which is estimated to be at most $\Delta E_{\rm d} = \pm 0.29$ keV at $E_{\rm d} = 10$ keV; thus, a negligible uncertainty in cross-section (at most 2.1%) is expected. Since the Coulomb explosion has been found to be "gentle" [11–16], the actual spread $\Delta E_{\rm d}$ should be significantly smaller. Indeed, the resulting thin-target $S(E)$

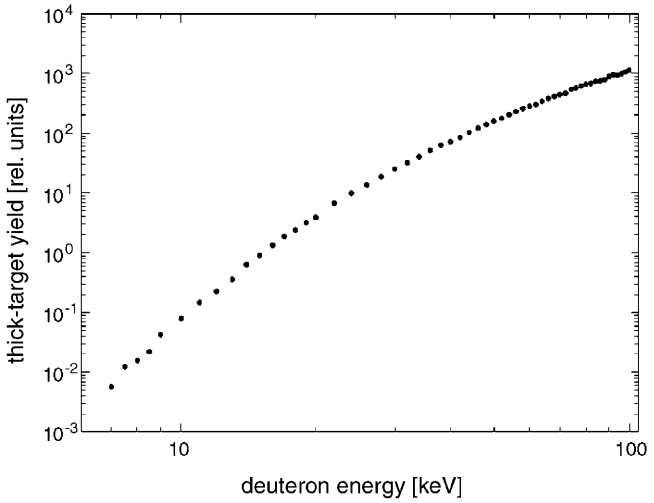

Fig. 4. Thick-target yield curve $Y^{\infty}(E_{\rm d},\theta)$ for protons from d(d, p)t as obtained in one run using an atomic (D_1^+) deuteron beam.

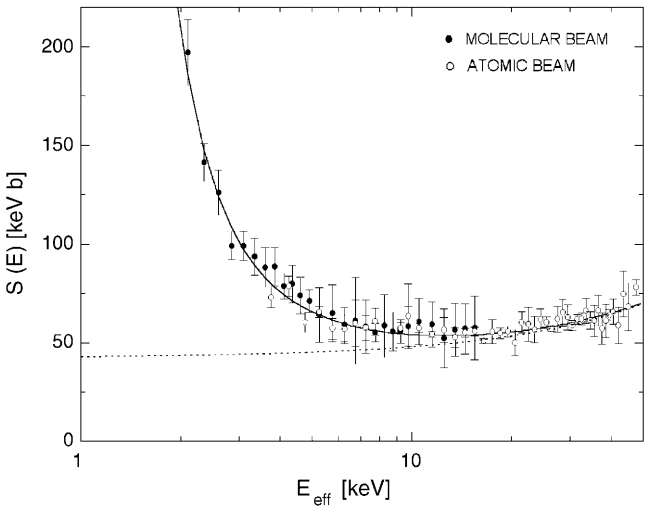

Fig. 5. Astrophysical $S(E)$ factor of d(d, p)t as obtained with a deuterated Ta foil (temperature = −10°C) for atomic (D_1^+) and molecular (D_3^+) deuteron beams. The errors shown arise predominantly from the spread of the (differentiated thick-target) thin-target yields from various runs. The dotted curve represents the bare $S(E)$ factor, while the solid curve includes the effects of electron screening with $U_{\rm e}$ = 309 eV.

factors (see below) displayed in fig. 5 are —within experimental uncertainties— identical for the atomic and molecular deuteron beams in the overlapping energy range and confirm the above expectation.

In order to arrive at a thin-target yield curve $Y(E_0,\theta)$, the thick-target yield curves (*e.g.*, fig. 4) were differentiated, *i.e.* the yield difference between two adjacent points $Y^{\infty}(E_0,\theta)$ and $Y^{\infty}(E_0-\Delta E_{\rm d},\theta)$ was calculated and divided by $\Delta E_{\rm d}$, to correct for variations in the energy step:

$$Y(E_0,\theta)=(Y^{\infty}(E_0,\theta)-Y^{\infty}(E_0-\Delta E_{\rm d},\theta))/\Delta E_{\rm d}\,. \quad (5)$$

For small energy steps, the quantities $K_{\Omega}(E,\theta)$, $W(E,\theta)$, and $\varepsilon_{\rm eff}(E)$ are approximately constant over $\Delta E_{\rm d}\equiv\Delta$, and the above equations simplify to

$$Y(E_0,\theta)=\Delta^{-1}\Omega K_{\Omega}(E_0,\theta)W(E_0,\theta) \times\varepsilon_{\rm eff}(E_0)^{-1}\int_{E_0-\Delta}^{E_0}\sigma(E){\rm d}E\,. \quad (6)$$

Since $\sigma(E)$ is not constant over Δ, one can define an effective energy $E_{\rm eff}$ within the energy step Δ, at which one-half of the reaction yield is obtained [1]:

$$Y(E_0,\theta)=\Omega K_{\Omega}(E_0,\theta)W(E_0,\theta)\varepsilon_{\rm eff}(E_0)^{-1}\sigma(E_{\rm eff})\,. \quad (7)$$

Since the product $K_{\Omega}(E_0,\theta)W(E_0,\theta)$ at $\theta=130°$ is energy independent to within 1% at the energy range $E_{\rm d}$ = 4 to 100 keV [3,6], we arrive at

$$Y(E_0,\theta)=\alpha\varepsilon_{\rm eff}(E_0)^{-1}\sigma(E_{\rm eff})\,, \quad (8)$$

with the constant $\alpha=\Omega K_{\Omega}(E_0,\theta)W(E_0,\theta)$. The effective stopping power $\varepsilon_{\rm eff}(E_0)$ for the Ta_xD target is given by the expression [1]

$$\varepsilon_{\rm eff}(E_0)=\varepsilon_{\rm D}(E_0)+x\varepsilon_{\rm Ta}(E_0)\,, \quad (9)$$

where $\varepsilon_{\rm D}(E_0)$ and $\varepsilon_{\rm Ta}(E_0)$ are the stopping powers (in units of eV atom^{-1}cm^2) of deuterium and tantalum, respectively, and x is the stoichiometric ratio. Since compilations on hydrided metals report [17] a minimum value of $x=2$, this value was adopted (see however below) together with SRIM [9] to arrive at $\varepsilon_{\rm eff}(E_0)$. It turned out that the energy dependence of $\varepsilon_{\rm eff}(E_0)$ is identical with $\varepsilon_{\rm Ta}(E_0)$ to within 1%; thus, the deduced energy dependence of $\sigma(E_{\rm eff})$ from eqs. (8) and (9) is within 1% independent of the assumed x value (for $x\geqslant 2$).

4 Results and discussion

The resulting cross-section $\sigma(E_{\rm eff})$, *i.e.* the weighted average of all runs, is illustrated in fig. 5 in form of the astrophysical $S(E_{\rm eff})$ factor and numerical values are summarised in table 1; the errors quoted arise predominantly from the spread of the (differentiated thick-target) thin-target yields from various runs. The absolute scale was obtained by normalisation to previous work [3] in the energy range $E_{\rm d}$ = 80 to 100 keV, where effects of electron screening are negligible. The normalisation led to a Ta_xD target stoichiometry with $x=7.9\pm1.0$.

In the analysis of the data shown in fig. 5, we assumed a bare $S(E)$ factor linearly increasing with energy, $S_{\rm b}(E)=S_{\rm b}(0)+mE$, consistent with previous work [3] and a recent microscopic calculation [18] predicting $S_{\rm b}(E)=53+0.48E$ keV b in the relevant energy range (E in keV). Relative to this function, the data were fitted with the enhancement factor of eq. (2) involving $U_{\rm e}$. A χ^2-fit including $S_{\rm b}(0)$, m, and $U_{\rm e}$ as free parameters led to χ^2(normalised)= 0.67, $S_{\rm b}(0)=43\pm1$ keV b, $m=0.54\pm0.05$ b, and $U_{\rm e}=309\pm12$ eV (quoted errors = one standard deviation), in good agreement with a previous observation $U_{\rm e}=322\pm15$ eV [6]. Thus, the

Table 1. Astrophysical $S(E)$ factor for d(d, p)t in deuterated Ta.

$E_{\rm eff}^{(a)}$ (keV)	$S(E)^{(b)}$ (keV b)	$E_{\rm eff}^{(a)}$ (keV)	$S(E)^{(b)}$ (keV b)
atomic beam (D_1^+)			
3.75	73 ± 5	22.5	60 ± 9
4.25	79 ± 5	23.5	57 ± 7
4.75	61 ± 5	24.5	62 ± 5
5.25	66 ± 3	25.5	60 ± 3
5.75	57 ± 5	26.5	57 ± 1
6.25	57 ± 7	27.5	62 ± 7
6.75	60 ± 12	28.5	65 ± 7
7.25	58 ± 6	29.5	63 ± 7
7.75	61 ± 7	30.5	59 ± 3
9.25	57 ± 3	31.5	62 ± 3
9.75	64 ± 16	32.5	62 ± 3
10.5	58 ± 2	33.5	66 ± 6
11.5	54 ± 1	34.5	62 ± 4
12.5	57 ± 6	35.5	61 ± 8
13.5	53 ± 5	36.5	66 ± 8
14.5	55 ± 2	37.5	57 ± 8
15.5	56 ± 2	38.5	61 ± 8
16.5	51 ± 1	39.5	64 ± 3
17.5	56 ± 6	40.5	66 ± 6
18.5	55 ± 3	42.0	59 ± 9
19.5	56 ± 3	43.5	75 ± 12
20.5	50 ± 7	45.0	68 ± 12
21.5	60 ± 5	47.5	78 ± 4
molecular beam (D_3^+)			
2.10	197 ± 17	6.25	59 ± 9
2.35	141 ± 10	6.75	61 ± 22
2.60	126 ± 11	7.25	58 ± 14
2.85	99 ± 7	7.75	55 ± 5
3.10	99 ± 7	8.25	59 ± 16
3.35	94 ± 9	8.75	56 ± 10
3.60	88 ± 10	9.25	56 ± 6
3.85	89 ± 10	9.75	58 ± 10
4.10	79 ± 6	10.5	61 ± 12
4.35	80 ± 10	11.5	59 ± 11
4.60	74 ± 9	12.5	52 ± 15
4.90	71 ± 6	13.5	57 ± 13
5.25	64 ± 14	14.5	57 ± 13
5.75	65 ± 14	15.5	58 ± 16

(a) Effective center-of-mass energy.
(b) Normalised to previous work [3] at $E_{\rm eff} \geqslant 40$ keV.

electron screening effect of d(d, p)t in deuterated Ta is indeed about one order of magnitude larger than in a gas target and must arise, therefore, predominantly from the deuteron environment in the Ta matrix. In this context several effects should be taken into consideration.

4.1 Stopping power at energies below the Bragg peak

It should be pointed out that the quoted $U_{\rm e}$ value depends on the energy dependence of the stopping power values of D in Ta at energies far below the Bragg peak ($E_{\rm d} = 300$ keV), where no energy loss data exist and the values derived from the compilation SRIM [9] are based on extrapolations at $E_{\rm d} \leqslant 100$ keV. Although it appears unlikely that the stopping power drops exactly with the inverse function of eq. (2), one cannot rule out rigorously this possibility. A direct measurement of stopping power values at ultra-low energies in deuterated Ta is a challenge to the experimentalist.

4.2 Thermal motion of target atoms

In the analysis of all previous experiments on electron screening, the target atoms were assumed to be at rest. However, in reality they have a kinetic energy $E_{\rm t}$, with $E_{\rm t} = kT$ for gases (T = gas temperature) and $E_{\rm t} = 0.5E_{\rm vib}$ for solids ($E_{\rm vib}$ = vibrational energy). This leads to a Doppler energy spread in the laboratory system [1, 19]

$$\Delta E_{\rm D} = 4(\ln 2 m_{\rm p} m_{\rm t}^{-1} E_{\rm t} E_{\rm p})^{1/2}\,, \qquad (10)$$

where $m_{\rm p}$ and $m_{\rm t}$ are the respective masses of projectile and target nuclides and $E_{\rm p}$ is the projectile energy. Note that the Doppler spread was discussed in the literature predominantly in connection with narrow resonances but not with a non-resonant process. Folding the energy spread $\Delta E_{\rm D}$ with the steeply dropping cross-section (eq. (1)) leads to an effective energy higher than $E_{\rm p}$, where the resulting energy increment is equivalent to a screening potential energy scaling —according to eq. (10)— with $E_{\rm p}^{1/2}$ or $E^{1/2}$. The resulting Doppler enhancement factor, $f_{\rm D}(E) \propto \exp(\text{const}\ U_{\rm e}/E^{3/2}) \propto \exp(\text{const}\ \Delta E_{\rm D}/E^{3/2}) \propto \exp(\text{const}/E)$, has a reduced energy dependence compared to eq. (2), $f_{\rm lab}(E) \propto \exp(\text{const}/E^{3/2})$; however, this reduced energy dependence has not been observed (*e.g.*, fig. 5).

Furthermore, for the ^{3}He(d, p)^{4}He reaction using a gas target at room temperature, the lowest energy $E = 5.0$ keV led to an observed cross-section enhancement $f_{\rm lab} = 1.9$. For these parameters, eq. (10) leads to $\Delta E_{\rm D} = 43$ eV corresponding to an effective beam energy increased by 1 eV and a cross-section enhanced by 0.3%. The d(d, p)t reaction using a deuterated Ta target at $E = 2.1$ keV leads to $f_{\rm lab} = 4.6$ (fig. 5); assuming a value of $E_{\rm t} = 1$ eV due to the lattice vibrations, one finds $\Delta E_{\rm D} = 88$ eV corresponding to a beam energy increment of 1.2 eV and a cross-section enhancement of 0.1%.

4.3 Channeling

A relevant difference between a gas target and a solid target is that the latter could in principle exhibit channeling effects: the deuteron beam being guided by the lattice into planes or axes, whereby an interstitial atom such as deuterium could be hit with an increased probability. The critical angle for channeling scales with the inverse square root of the incident energy and the channeled flux scales, thus, with the inverse of the incident energy. Thus, one may expect an enhancement factor in the cross-section due to channeling proportional to $1/E$, which is however

not observed (fig. 5). Furthermore, the random orientation of the Ta matrix in the experiments as well as radiation damage of the crystalline structure by the intense deuteron beam lead to large dechanneling effects. It is concluded therefore that the channeling phenomenon is not the primary cause of the large observed cross-section enhancements in deuterated Ta. A similar conclusion was reached recently by Czerski *et al.* [20].

4.4 Diffusion and conductivity

It was also suggested recently [20] that the diffusion property or the conductivity of the Al, Zr, and Ta materials may give a hint on the large enhancements. However, no consistent picture arose: the diffusion coefficient for Zr is at least 3 orders of magnitude smaller than that for Al and Ta, while the reported U_e values [6] do not reflect such a trend; similarly, the conductivity of Zr is at least a factor 3 smaller than that for Al and Ta.

4.5 A special potential well?

It may be of interest to note that a fusion of D with Ta would lead to a screening potential energy of about $U_{ad} = 2$ keV, in the adiabatic limit. If the electron clouds of the Ta atoms in the lattice would be such that about 10% of them form a potential well around the interstitial D atom, one might arrive at a possible explanation. One must await however the results of detailed calculations, although some theoretical work in this direction has been already performed [21–24].

5 Summary

None of the suggested scenarios have provided yet an answer to explain the large enhancement in cross-section for d(d, p)t in Ta and in other materials. Since previous work [6] found U_e values decreasing with the nuclear charge of the metals, it appears desirable to confirm this trend for Al and Zr but also to study other metals such as Ti, Cu, Pd, and Au. Furthermore, non-metallic targets such as diamond and silicon should be used to elucidate the question whether the large screening effects occur only in metals (see however [19]). Finally, other ion beams in deuterated or hydrated materials should exhibit similar large screening effects, such as the d(^{3}He, p)^{4}He or ^{1}H(^{7}Li, α)^{4}He reactions.

We thank D. Israel and M. Beck for assistance during part of the experiments. The help of the technical team at the Dynamitron-Tandem-Laboratorium is highly appreciated. Finally, we thank G. Dollinger and his team (Technische Universität München) for the ERDA analysis of one sample. This work has been supported in part by BMBF (06BO812 and 05CL1PC1/1), DFG (436UNG113-146), and OTKA(T034259).

References

1. C. Rolfs, W.S. Rodney, *Cauldrons in the Cosmos* (University of Chicago Press, 1988).
2. H.J. Assenbaum, K. Langanke, C. Rolfs, Z. Phys. A **327**, 461 (1987).
3. U. Greife, F. Gorris, M. Junker, C. Rolfs, D. Zahnow, Z. Phys. A **351**, 107 (1995).
4. M. Aliotta, F. Raiola, G. Gyürky, A. Formicola, R. Bonetti, C. Broggini, L. Campajola, P. Corvisiero, H. Costantini, A. D'Onofrio, Z. Fülöp, G. Gervino, L. Gialanella, A. Guglielmetti, C. Gistavino, G. Imbriani, M. Junker, P.G.P. Moroni, A. Ordine, P. Prati, V. Roca, D. Rogalla, C. Rolfs, M. Romano, F. Schümann, E. Somorjai, O. Straniero, F. Strieder, F. Terrasi, H.P. Trautvetter, S. Zavatarelli, Nucl. Phys. A **690**, 790 (2001).
5. F. Strieder, C. Rolfs, C. Spitaleri, P. Corvisiero, Naturwiss. **88**, 461 (2001).
6. K. Czerski, A. Hulke, A. Biller, P. Heide, M. Hoeft, G. Ruprecht, Europhys. Lett. **54**, 449 (2001).
7. H. Yuki, J. Kasagi, A.G. Lipson, T. Ohtsuki, T. Baba, T. Noda, B.F. Lyakhov, N. Asami, JETP Lett. **68**, 823 (1998).
8. A. Krauss, H.W. Becker, H.P. Trautvetter, C. Rolfs, K. Brand, Nucl. Phys. A **465**, 150 (1987).
9. H. Andersen, J.F. Ziegler, *The Stopping and Ranges of Ions in Matter* (Pergamon, New York, 1977) and SRIM-2000.
10. J.C. Barbour, B.L. Doyle, *Handbook of Modern Ion Beam Materials*, edited by J.R. Tesmer, N. Nastasi (Materials Research Society, 1995) p. 83; G. Dollinger, T. Faestermann, P. Maier-Komor, Nucl. Instrum. Methods B **64**, 422 (1992).
11. B. Meierjohann, W. Seibt, Z. Phys. **225**, 9 (1969).
12. B. Meierjohann, M. Vogler, J. Phys. B **9**, 1801 (1976).
13. M. Vogler, W. Seibt, Z. Phys. **210**, 337 (1968).
14. M. Vogler, B. Meierjohann, Z. Phys. A **283**, 11 (1977).
15. M. Vogler, B. Meierjohann, J. Chem. Phys. **69**, 2450 (1978).
16. F. Raiola, G. Gyürky, M. Aliotta, A. Formicola, R. Bonetti, C. Broggini, L. Campajola, P. Corvisiero, H. Costantini, A. D'Onofrio, A. Formicola, Z.Fülöp, G. Gervino, L. Gialanella, A. Guglielmetti, C. Gistavino, G. Imbriani, M. Junker, R.W. Kavanagh, P.G.P. Moroni, A. Ordine, P. Prati, V. Roca, D. Rogalla, C. Rolfs, M. Romano, F. Schümann, E. Somorjai, O. Straniero, F. Strieder, F. Terrasi, H.P. Trautvetter, S. Zavatarelli, Eur. Phys. J. A **10**, 487 (2001).
17. W.M. Mueller, J.P. Blackedge, G.G. Libowitz, *Metal Hydrides* (Academic Press, New York, 1968).
18. H.M. Hofmann, Universität Erlangen, private communication (2001).
19. H. Bethe, G. Placzek, Phys. Rev. **51**, 450 (1937).
20. K. Czerski, A. Huke, P. Heide, G. Schiwietz, preprint, Technische Universität Berlin, 2001.
21. S. Ichimaru, Rev. Mod. Phys. **65**, 252 (1993).
22. A.J. Legett, G. Baym, Phys. Rev. Lett. **63**, 191 (1989).
23. M. Rambaut, Phys. Lett. A **164**, 155 (1992).
24. V.A. Kirkinskii, Y.A. Novikov, Europhys. Lett. **46**, 448 (1999).